Published in final edited form as:
*Neuroscience*. 2010 November 10; 170(4): 992–1003. doi:10.1016/j.neuroscience.2010.08.034.

# Specific Disruption of Astrocytic $Ca^{2+}$ Signaling Pathway *in vivo* by Adeno-Associated Viral Transduction

**Yicheng Xie**[1,2], **Tiannan Wang**[1], **Grace Y. Sun**[3], and **Shinghua Ding**[1,2,*]

[1]Dalton Cardiovascular Research Center, University of Missouri-Columbia, MO 65211

[2]Dept. of Biological Engineering, University of Missouri-Columbia, MO 65211

[3]Dept. of Biochemistry, University of Missouri-Columbia, MO 65211

## Abstract

Astrocytes are the predominant glial-cell type in the central nervous system (CNS) and they are known to play an active role in modulating neuronal function. Since many of the same molecules including G-protein coupled receptors (GPCRs) are expressed in both neurons and astrocytes, *in vivo* pharmacological manipulations to target astrocytes lack specificity. In this study, we investigated the effect of Pleckstrin Homology (PH) domain of Phospholipase C (PLC)-like protein p130 (p130PH) on $Ca^{2+}$ signaling in astrocytes *in vivo*. We used the serotype 2/5 recombinant adeno-associated virus (rAAV2/5) vectors to introduce p130PH fused with a tagged protein monomer red fluorescent protein at the N-terminal (i.e., transgene mRFP-p130PH). In order to selectively disrupt the $Ca^{2+}$ signaling pathway in astrocytes, the transgene was driven by a novel astrocyte-specific promoter gfa$ABC_1D$. Our results show that mRFP-p130PH is exclusively expressed in astrocytes with a high efficiency and a stable expression level. *In vivo* imaging using two-photon microscopy demonstrated reduced $Ca^{2+}$ signal in transduced astrocytes in response to ATP stimulation. As $Ca^{2+}$ signaling is a characteristic form of cellular excitability in astrocytes that can mediate chemical transmitter release and contribute to neuronal excitotoxicity, the current study provides an *in vivo* approach to better understand $Ca^{2+}$-dependent gliotransmission and its involvement in glia-related diseases.

### Keywords

Adeno-associated virus; glial promoter; $Ca^{2+}$ signaling; two-photon imaging

## INTRODUCTION

Astrocytes exhibit cellular excitability through $Ca^{2+}$ signaling mediated by the activation of a variety of G-protein coupled receptors (GPCRs), including P2Y receptors (Erb et al., 2006), metabotropic glutamate receptors (mGluRs), gamma-aminobutyric acid ($GABA_B$) receptors, and dopamine receptors (Haydon and Carmignoto, 2006; Ni et al., 2007). These receptors are coupled to downstream pathways involving phospholipase C (PLC) and



*Correspondence should be addressed to S.D. (dings@missouri.edu), Dalton Cardiovascular Research Center, Dept. of Biological Engineering, University of Missouri-Columbia, 134 Research Park Drive, Columbia, MO 65211. Tel: (573)884-2489.

liberation of inositol 1,4,5-trisphosphate ($IP_3$), a second messenger responsible for $Ca^{2+}$ release from endoplasmic reticulum (ER) through activation of $IP_3$ receptors ($IP_3Rs$) expressed. Studies with cultured astrocytes (Parpura et al., 1994) as well as with brain slice preparations (Fellin et al., 2004; D'Ascenzo et al., 2007; Angulo et al., 2004) have linked the increase in astrocytic $Ca^{2+}$ to the release of chemical transmitters. Thus, $Ca^{2+}$ signaling in astrocytes serves as a mediator of bidirectional interactions between neurons and astrocytes. Astrocytic $Ca^{2+}$ signaling also plays a role in neuronal death under pathological conditions. For example, enhanced $Ca^{2+}$ signaling in astrocytes following status epilepticus has been shown to contribute to neuronal excitotoxicity, presumably through glutamate release (Ding et al., 2007). Activation of group I mGluR in astrocytes by dihydroxyphenylglycine (DHPG) increased the water permeability of aquaporin-4 channels via protein kinase G-mediated phosphorylation and subsequently caused edema following ischemia (Gunnarson et al., 2008). However, studies to understand the function of astrocytic $Ca^{2+}$ elevation induced by pharmacological reagents have been problematic because many of the same GPCRs are expressed in both neurons and astrocytes. To further advance knowledge regarding neuron-glia interactions and to explore the role of astrocytic $Ca^{2+}$ signaling in neurodegeneration, it is important to develop a cell-type specific approach that can selectively modulate $Ca^{2+}$ signaling in astrocytes within the brain.

Currently, there are two approaches to knockout and introduce genes *in vivo*. The first is to generate knockout and transgenic mice, which is expensive and time consuming. In many instances, knockout and introduction of genes are embryonic lethal and may cause developmental defects in mice. Although transgenic and knockout mice have been generated to manipulate astrocytic $Ca^{2+}$ signaling (Fiacco et al., 2007; Li et al., 2005), viral transduction provides an alternative approach for gene delivery *in vivo*. This approach is increasingly used to introduce foreign genes into the nervous system because many types of viruses can deliver genes to the non-dividing cells, which include neurons in the brain (Davidson and Breakefield, 2003). Viral transduction provides a flexible approach for delivering genes to brain regions. Furthermore, using a cell-type-specific promoter, it is feasible to selectively deliver genes to a specific type of cells *in vivo*. Our goal in this study is to use a viral approach to selectively disrupt the PLC/$IP_3$ $Ca^{2+}$ signaling pathway in astrocytes. Through this approach, we will test whether transgene expression could reduce receptor-mediated $Ca^{2+}$ elevation in astrocytes *in vivo*. Using the recombinant adeno-associated virus (rAAV), we introduced the Pleckstrin Homology domain of PLC-like protein p130 (p130PH) into astrocytes to disrupt the $Ca^{2+}$ signaling pathway. The p130PH can act as a mobile cytosolic $IP_3$ buffer to inhibit $Ca^{2+}$ release from internal store (Lin et al., 2005). rAAV vectors were chosen because they are highly effective for gene delivery. These vectors are non-pathogenic and can express a transferred gene for the life of the animal (Cearley and Wolfe, 2006). To achieve astrocyte-specific expression of p130PH, we inserted a recently-cloned glial fibrillary acidic protein (GFAP) promoter, gfa$ABC_1D$ (Lee et al., 2008), into a *cis* cloning plasmid. Pseudo-type 2/5 rAAV (rAAV2/5) vectors with a serotype 2 AAV (AAV2) *rep* and a serotype 5 AAV (AAV5) *cap* gene were produced. These vectors were then injected into the somatosensory cortex of mouse brains. p130PH expression profiles were assessed by directly visualizing the fluorescence of the fusion protein in brain sections. The functional consequence of the transgene was further evaluated by *in vivo* $Ca^{2+}$ imaging using two-photon (2-P) microscopy.

## Experimental Procedures

### Cultured astrocytes and DNA transfection

Primary cortical astrocytes from 1 to 2 day-old rat brains were prepared using a standard stratification/cell-shaking procedure (McCarthy and de Vellis, 1980). This procedure yielded confluent mixed glial cultures within 7–9 d, after which the flasks were shaken at 180 rpm at

room temperature for 3 hr to remove microglial cells. These astrocytes (>95% as quantified by the anti-glial fibrillary acidic protein, GFAP) were subsequently subcultured at 37°C in a 5% $CO_2$ humidified incubator and fed every 48 hr with fresh Dulbecco's Modified Eagle Medium (DMEM) containing 10% fetal bovine serum (FBS) as described previously (Zhu et al., 2006). Astrocytes used for imaging were cultured on glass coverslips and were transfected with DNA plasmids containing transgene mRFP-p130PH (i.e., p130PH fused with a monomer red fluorescent protein at the N-terminal, kindly provided as a gift by Dr. Gyorgy Hajnoczky, Thomas Jefferson University, Philadelphia) using FuGENE 6 transfection reagent (Roche Diagnostics, IN) according to the manufacturer's instructions. Astrocytes transfected with mRFP were used as a control for viral transduction.

### $Ca^{2+}$ imaging in cultured astrocytes

For $Ca^{2+}$ imaging in astrocytes, cells were cultured on glass cover slips and incubated for 45 min with 0.5 ml fluo-4 AM (1μg/ml, diluted from a stock solution of 1μg/μl prepared with dimethyl sulfoxide (DMSO)) in artificial cerebral spinal fluid (ACSF) (in mM): 120 NaCl, 10 Hepes, 3.1 KCl, 2 $CaCl_2$, 1.3 $MgCl_2$, and 10 glucose (pH 7.4). After incubation, excess fluo-4 AM was washed with ACSF. Time-lapse $Ca^{2+}$ imaging was performed using an upright wide-field epi-fluorescence microscope (FN1 system, Nikon) with a 40×/0.8 water immersion objective. Excitation was generated with an X-Ford metal halide lamp filtered with a fluo-4 filter cube. Emission was detected by a CoolSNAP-EZ CCD-camera (Photometrics, AZ). ATP (20 μM) was applied through a perfusion system equipped with a pinch valve that can control the duration of application.

### Surgical craniotomy and *in vivo* 2-photon $Ca^{2+}$ imaging in astrocytes

Male FVB/NJ mice 5–7 weeks of age were purchased from The Jackson Laboratory (Bar Harbor, ME). All procedures were performed in accordance with the "NIH Guide for Care and Use of Laboratory Animals", and were approved by the University of Missouri Animal Care Quality Assurance Committee. Detailed procedures for surgery and *in vivo* imaging have been described in our previous publications (Ding et al., 2007; Ding et al., 2009). Briefly, mice were anesthetized with an intraperitoneal (IP) injection of urethane (1.5–2.0 mg/g body weight) dissolved in ACSF. A circular craniotomy (2.0 mm in diameter) was made using a high speed drill over the somatosensory cortex at coordinates −0.8 mm from the bregma and 2.0 mm lateral to the midline. A custom-made metal frame was attached to the skull with cyanocrylate glue, and the dura was then carefully removed with fine forceps. For loading of the $Ca^{2+}$ indicator fluo-4 into astrocytes, fluo-4 AM was dissolved in pluronic acid (20% pluronic acid plus 80% DMSO) to obtain a 10 μg/μl stock solution. This stock solution (2.5 μl) was mixed with 40 μl ACSF and applied to the dura-free cortical surface within the craniotomy for 1 hr. Mice were transferred to the stage of a 2-P microscope for *in vivo* imaging. Images were obtained using a Leica SP 1500 microscope using a 60×/0.9 water immersion objective. A Mai Tai laser (Spectra-Physics, CA) was used for 2-P excitation (820 nm). For ATP administration, ACSF containing 0.5 mM ATP was applied to the cortex. The cranial window was then refilled with 2% agarose containing 0.5 mM ATP. ACSF containing same concentration of ATP was applied on the surface of solidified agarose before imaging. Imaging was usually performed on astrocytes 80–100 μm below the cortical surface within 15–60 min after ATP administration. Multiple time-lapse imaging experiments were performed to monitor $Ca^{2+}$ signals for a period of 7.5 min for each time-lapse imaging experiment with an acquisition rate of one image frame every two seconds. For each animal, 15–25 astrocytes in 4–5 fields were imaged and all the astrocytes imaged were used for analysis. Throughout the experiment (about 3–4 hr from the beginning of surgery to the end of imaging), the mice were maintained at 37°C using a heating pad (Fine Science Tool, CA) and kept at a surgical level of anesthesia.

### Construction of *cis* expressing plasmid and production of rAAV vectors

To construct a *cis* expressing plasmid that has an astrocyte-specific GFAP promoter and the gene of interest, the cytomegalovirus (CMV) promoter of the *cis* cloning plasmid pZac2.1 was swapped by a 681 bp GFAP promoter gfaABC$_1$D (Lee et al., 2008) using Bgl II on the 5' end and EcoR I on the 3' end. The transgene mRFP-p130PH or mRFP alone was inserted into cloning sites to form a new expressing plasmid pZac2.1-gfaABC$_1$D-mRFP-p130PH or pZac2.1-gfaABC$_1$D-mRFP (Fig. 2A). The p130PH had been previously cloned to study membrane localization of the PH domain (Varnai et al., 2002). The plasmid included a SV40 late-polyadenylation signal sequence (Poly A). The transgene and Poly A were flanked by inverted terminal repeats (ITRs). The constructs were sequenced to confirm the correct insertions of the promoter and transgene. rAAV vectors were produced by triple transfection of Human Embryonic Kidney 293 (HEK 293) at the University of Pennsylvania Gene Therapy Program Vector Core and showed a titer of $8\times10^{12}$ genomic copies (GC) per ml. Briefly, this *cis* plasmid was cotransfected with an AAV *trans* plasmid and an adenoviral helper plasmid in HEK 293 cells to produce the pseudo-type rAAV2/5 vectors. The vectors were purified using a method based on buoyant density (cesium chloride) ultracentrifugation and were collected in 5% glycerol of phosphate-buffered saline (PBS) (Fisher et al., 1997). Vectors were stored in aliquots at −80 °C and thawed on ice before use.

### Viral injection into the mouse cortex

Mice (5–7 weeks of age) were anesthetized with ketamine/xylazine. A skin incision was made and a small hole (0.2 mm diameter) was drilled in the skull for injection into the barrel cortex and hippocampus. The cortical region was chosen because of easy assess to study transgene function *in vivo* using 2-P microscopy. rAAV vectors (1 μl) were injected with a nanoliter injector (Drummond Scientific Company, PA) through the hole at a rate of 4 nl/s using a glass pipette with a 10–15 μm-diameter tip. The skin was sutured after injection and mice were maintained at the animal facility after recovery.

### Transcardial perfusion and histo- and immunocyto-chemistry studies

The procedure for transcardial perfusion has been previously described (Ding et al., 2007). Briefly, mice were anesthetized with halothane and transcardially perfused first with ice-cold PBS and then 4% paraformaldehyde (PFA) in PBS (pH=7.4). After perfusion, the brain was post-fixed with 4% PFA at 4°C overnight, and then transferred to 30% sucrose for 2–3 days to prevent ice crystal formation. Coronal brain sections (thickness 20 μm) were cut on a cryostat (Leica CM 1900), and were collected serially on pre-cleaned slides or placed into a 48-well plate with PBS. Neuronal Nuclei (NeuN) staining for neurons has also been previously described (Ding et al., 2007). Briefly, brain sections were incubated with rabbit anti-NeuN (1:1000, Millipore) overnight, and subsequently incubated with fluorescein isothiocyanate (FITC)-conjugated goat anti-rabbit immunoglobulin G (IgG) (1:100, Millipore, CA) for 2 hr. Similar procedures were used for staining of GFAP, the ionized calcium-binding adaptor molecule 1 (Iba1), CNPase and NG2 using rabbit polyclonal anti-GFAP (1:150, Sigma), rabbit anti-Iba1 (1:600, Wako Chemicals USA, VA), mouse anti-CNPase (1:100, Millipore) and rabbit anti-NG2 (1:200, Millipore) antibodies using FITC- or rhodamine-conjugated anti-rabbit and anti-mouse IgG as secondary antibodies. Nuclei were stained with 4',6-diamidino-2-phenylindole (DAPI) (0.5 μg/ml in PBS) in anti-fade mounting medium (Invitrogen, CA). Stained sections were viewed with an Olympus FV1000 laser scanning confocal fluorescence microscope and analyzed using the MetaMorph imaging program (Universal Imaging, CA). All experiments for immunostaining except those in Fig. 6 were performed using mice 2–3 weeks after viral injection. For immunostaining to study glial activation (i.e., GFAP and Iba1 staining) after viral injection, brain sections with needle track were chosen based on visual inspection. To

study colocalization of transgene with other markers, brain sections without needle track were chosen for immunostaining.

### Data analysis of the $Ca^{2+}$ signal

For *in vivo* $Ca^{2+}$ imaging in astrocytes, data analysis were described in our previous studies (Ding et al., 2009; Ding et al., 2007). Briefly, the fluorescent signals were quantified by measuring the mean pixel intensities of the cell body of each astrocyte using the MetaMorph software (Universal Imaging, CA). $Ca^{2+}$ changes were expressed as $\Delta F/Fo$ values vs. time, where $Fo$ was the baseline fluorescence. To calculate the magnitude of $Ca^{2+}$ signals without subjective selection of threshold values, we integrated the $\Delta F/Fo$ signal over the imaging period and normalized to 300 s using the Origin software (OriginLab Corporation, MA). The resulting value was expressed as $\Delta F/Fo.s$. Data collected from multiple cells from each mouse were averaged and the averaged value of these cells was then used as a single value for individual mice. The summary data were the average value from multiple mice. A similar method was used for the analysis of $Ca^{2+}$ signals in cultured astrocytes. The magnitude of $Ca^{2+}$ signals were determined by the integration of $\Delta F/Fo$ over the time period of $Ca^{2+}$ increase after ATP stimulation.

### Cell counting

The number of S100β+, GFAP+, mPFP-p130PH+ and NeuN+ cells in the cortex and hippocampus were counted from maximal projection images. Cells were counted if they contained a whole cell body (Liu et al., 2009). The number was presented as per $mm^2$.

### Statistics

Data are reported as mean ± SEM. Statistical comparisons of data between two groups of experiment were made by a Student's *t*-test. $p<0.05$ was considered to be statistically significant.

## RESULTS

### Expression of p130PH attenuates ATP-induced $Ca^{2+}$ signaling in primary astrocytes

$Ca^{2+}$ elevations in astrocytes are predominantly mediated by the Gq-linked GPCR signaling pathway (Petravicz et al., 2008; Haydon, 2001), and it is reasonable to hypothesize that the expression of p130PH in astrocytes may attenuate a $IP_3$ receptor-mediated $Ca^{2+}$ release from the ER. Previously, studies with cultured astrocytes as well as astrocytes *in vivo* provided evidence that ATP could stimulate $Ca^{2+}$ elevations through activation of P2Y receptors (Haydon, 2001; Ding et al., 2007; Tian et al., 2005; Erb et al., 2006). In this study, we initially tested the role of p130PH in $Ca^{2+}$ inhibition by transient expression of this protein in primary cultured rat astrocytes, using live cell $Ca^{2+}$ imaging with ATP stimulation. The transfected and non-transfected cells can be differentiated by the tag protein mRFP. A subset of astrocytes was expressed with mRFP 1 day after transfection. The fluorescence was uniformly distributed throughout the cytoplasm (Fig. 1a) and consistent with a previous study using COS-7 cells (Varnai et al., 2002). Application of ATP (20 μM) to non-transfected astrocytes resulted in robust $Ca^{2+}$ elevations, while astrocytes expressing mRFP-p130PH exhibited a reduction of 86±10 % following ATP stimulation (Fig. 1b–c). To determine whether transfection with mRFP itself affected $Ca^{2+}$ signaling, mRFP alone was expressed in astrocytes as an additional control. The average magnitudes of ATP-stimulated $Ca^{2+}$ signals were similar in mRFP-expressing cells as compared to non-transfected cells (Fig. 1c) demonstrating that reduction in the $Ca^{2+}$ signal in mRFP-p130PH-expressing astrocytes is due to the buffering of $IP_3$ by the p130PH protein.

### Selective expression of mRFP-p130PH in astrocytes *in vivo* using rAAV2/5 transduction

The main goal for this study is to inhibit $Ca^{2+}$ signaling in astrocytes *in vivo* using viral transduction to express p130PH. After demonstrating the utility of p130PH in reducing $Ca^{2+}$ signals in primary cultured astrocytes, we subcloned mRFP-p130PH into a *cis* rAAV-expressing plasmid. Selective expression of mRFP-p130PH in astrocytes was controlled by a novel GFAP promoter gfa$ABC_1D$ inserted in the construct (Fig. 2a). The gfa$ABC_1D$ promoter is a new version of gfa2 GFAP promoter, and since it is only 681 bp in size (Lee et al., 2008), it is possible to insert a relatively large transgene into the vector. rAAV2/5 vectors were prepared as this serotype has been suggested to have tropism for astrocytes (Halassa et al., 2007;Tenenbaum et al., 2004;Davidson et al., 2000).

At different times after viral injection into the barrel cortex, mice were sacrificed and transcardially perfused for histological study. At two weeks after injection, we were able to localize the transduced region in the cortex (after fixing with PFA) using epi-fluorescence microscopy (data not shown), indicating the successful expression of fusion protein mRFP. Confocal microscopy was used to directly visualize individual mRFP-p130PH-expressing cells in coronal brain sections. These cells have a bushy morphology with many fine terminal processes emanating from the primary processes (Fig. 2b–d), and resemble the morphology of astrocytes previously imaged *in vivo* (Ding et al., 2007;Nimmerjahn et al., 2004;Wilhelmsson et al., 2006). This observation suggests specific expression of transgene mRFP-p130PH in astrocytes driven by the gfa$ABC_1D$ promoter. From a single optical section image, many black spots, i.e., small round areas with low fluorescent intensity (Fig. 2c, marked with *) were observed. They were further identified as neurons using immunostaining of the neuronal marker NeuN (Fig. 3b). rAAV2/5 transduction resulted in broad distribution of mRFP+ cells throughout all cortical layers. Normally a region of 800×800 μm can be transduced around the middle of the injection site.

It has been shown that astrocytes are activated in response to CNS injury or disease, manifested by increased GFAP expression levels (Sofroniew, 2005). We evaluated whether AAV transduction could cause astrocyte activation using GFAP immunostaining. Fig. 2e and f show a transduced section with different resolutions stained with the GFAP antibody. Notably, astrocytes were highly expressed with GFAP in the dorsal surface of the cortex in the transduced region and were colocalized with mRFP signal. However, only a slight expression of GFAP was observed in the deep layers of the cortex where many cells were transduced and can be identified by mRFP fluorescence (Fig. 2e). In normal mice, astrocytes express low level of GFAP in the cortex (Wilhelmsson et al., 2006) in contrast to high GFAP expression in the hippocampal region. Therefore, our data suggest that the relatively high-level expression of GFAP in the dorsal surface of the transduced section might have been resulted from the activation of astrocytes caused by the injury of injection or by drilling at the injection site, but not by rAAV transduction *per se*. Thus, our results indicate that rAAV2/5 transduction did not cause astrocyte activation. Furthermore, immunostaining of Iba1, a marker for resting and activated microglia, indicates that microglia around the injection site exhibit a globoid morphology which is characteristic of activated microglia (Fig. 2g, middle panel). However, microglia in the transduced region, but distant from the injection site have normal morphology (Fig. 2h) as compared with the non-transduced region (data not shown) (Zhang et al., 2010). In addition, they have similar morphology in the dorsal surface and deep layer of the cortex (Fig. 2h). These results suggest that microglia activation around the injection site is due to mechanical injury and not by rAAV transduction *per se*.

In order to estimate viral transduction efficiency, the numbers of mRFP-expressing cells and GFAP+ cells were counted in the dorsal surface of the cortex within the transduced region. Our data show that 94.7±1.2% of the GFAP+ astrocytes expressed mRFP-p130PH in this

region (n= 7 sections from N=4 mice with a total of 155 in the cortex region). These results demonstrate the high efficiency of viral transduction and astrocyte-specific expression of the transgene driven by gfaABC$_1$D promoter.

Using immunostaining for S100β (another astrocyte-specific marker), we further confirmed that mRFP-p130PH is selectively expressed in astrocytes contained within the cortex (Fig. 3a). We also stained the transduced brain sections with antibodies against NeuN, Iba1, CNPase and NG2, which are specific protein markers for neurons, microglia, oligodendrocytes, and NG2 glial cells. In the entire transduced region, including the deep layers of the cortex, no co-localization of mRFP fluorescence with NeuN, Iba1, CNPase, and NG2 signal was observed (Fig. 3b–e). From the single optical section images, it is evident that neurons were surrounded by mFRP fluorescence (* in Fig. 3b). Thus we conclude that mRFP-p130PH is exclusively expressed with high efficiency in astrocytes driven by the gfaABC$_1$D promoter.

To test whether transgene expression in astrocytes using this serotype of AAV has a regional difference, we injected viral vectors into the hippocampus. Immunostaning data indicate the same results as those seen in the cortex, i.e., the exclusive expression of mRFP-p130PH in GFAP+ astrocytes, and not in NeuN+, Iba1+, CNPase+ and NG2+ cells (Fig. 4a, c, e, g, and i). This is further confirmed by orthogonal analysis of 3D confocal images (Fig. 4b, d, f, h, j). Astrocytes in the hippocampus express a high level of GFAP. Similar to the results from the cortex, we found that 93.2±0.8 % of GFAP+ cells are mRFP-p130PH+ in the hippocampal CA1 region (n= 6 brain sections from N=4 mice with a total of 357 astrocytes in the hippocampal CA1 region). On the other hand, we did not find any mRFP-p130PH+ cell to be GFAP negative. Thus our data demonstrate high efficiency of viral transduction and high specificity of transgene expression in astrocytes. When mRFP was expressed alone using viral transduction, the same results were obtained as compared with mRFP-p130PH (Fig. 5), i.e., mRFP is colocalized with S100β.

## Cellular toxicity and the time course of transgene expression

Many studies indicated no toxicity resulting from rAAV transduction in the CNS (Cearley and Wolfe, 2006; Davidson and Breakefield, 2003). Here, we tested the effects of our viral vectors and injection conditions on neuronal and glial toxicity. Results in Fig. 2e–h indicate that viral transduction *per se* did not cause activation of astrocytes and microglia. We further examined whether viral transduction would affect neuronal and astrocytic density at different time points after viral injection. Because NeuN+ cells represent healthy neurons, we counted the number of NeuN+ cells in layer 2/3 of the transduced and non-transduced cortical regions. The NeuN+ cell distribution within the transduced regions, but distant from injection site, was found to be uniform and similar in density compared to the non-transduced regions (Fig. 6a and b). In addition, NeuN+ cells remain the same density at different post-transduction time points (Fig. 6c). Since there are similar densities of NeuN+ cells in the transduced and non-transduced regions (Fig. 6c), these results indicate little or no neuronal toxicity induced by viral transduction.

We next examined the densities of transduced astrocytes at different time points after transduction. Using confocal microscopy, mRFP fluorescence signals were clearly visible in the cell body one week after viral transduction in the brain sections (Fig. 6e). However, the fluorescence was not revealed in the processes in a majority of transduced cells during this time point. We postulate that one week is not long enough to complete transgene expression in astrocytes *in vivo*. Between 2 and 10 weeks post-transduction, mRFP fluorescence signals were revealed in fine bush-like processes from the main cellular processes and terminating processes, i.e., “endfeet” (see arrow heads in Fig. 6f and g) wrapping around the blood vessel, a typical morphology of astrocytes *in vivo*. Our results show that the densities of

mRFP-p130PH-expressing astrocytes in the transduced regions were similar at different post-transduction time points (Fig. 6d). These results demonstrate stable expressions of the transgene in astrocytes with little cellular toxicity.

### Selective inhibition of $Ca^{2+}$ signal in astrocytes transduced with mRFP-p130PH *in vivo*

In order to test the functionality of mRFP-p130PH in transduced astrocytes in the brain, we performed *in vivo* $Ca^{2+}$ imaging using 2-P microscopy (Ding et al., 2009; Ding et al., 2007). We expect that mRFP-p130PH-expressing astrocytes would exhibit a reduced $Ca^{2+}$ signal in response to ATP stimulation. Astrocytes were labeled with fluo-4 AM using a surface application approach (Fig. 7a) (Ding et al., 2007). Utilizing 2-P microscopy, mRFP-p130PH-expressing astrocytes can be readily identified *in vivo* as deep as 100 μm from the cortical surface (Fig. 7b). Fig. 7c shows live imaging of a single optical section of 2-P image of mRFP-p130PH-expressing astrocytes labeled with the $Ca^{2+}$ indicator fluo-4. The merged images show that mRFP-p130PH fluorescence was colocalized with fluo-4 fluorescence, providing an additional piece of evidence that mRFP-p130PH is specifically expressed in astrocytes, as fluo-4 AM selectively label astrocytes *in vivo* using surface loading (Hirase et al., 2004; Wang et al., 2006; Takano et al., 2006; Ding et al., 2009; Ding et al., 2007). Astrocytes in the cortices of live mice is quiescent with spontaneous $Ca^{2+}$ activity, yet exhibited repetitive $Ca^{2+}$ oscillations expressed as waves in response to ATP stimulation (Ding et al., 2009; Ding et al., 2007) (Fig. 6d). Using ATP stimulation, we tested whether mRFP-130PH expression by viral transduction could inhibit ATP stimulated $Ca^{2+}$ signaling. When 0.5 mM ATP was applied on the cortical surfaces of transduced mouse brains, the mRFP-p130PH-expressing astrocytes exhibited a reduced $Ca^{2+}$ signal (Fig. 7e). Both the amplitude of individual $Ca^{2+}$ transients and the frequency of $Ca^{2+}$ oscillation were reduced in mRFP-p130PH-expressing astrocytes as compared to astrocytes in non-transduced mice (Fig. 7d and e). Overall, the average $Ca^{2+}$ signal in mRFP-p130PH-expressing astrocytes was reduced by 71 % compared with control astrocytes (Fig. 7f). The magnitude of the ATP-induced $Ca^{2+}$ signal from astrocytes expressing mRFP alone by viral transduction is similar to control astrocytes from non-transduced mice (Fig. 7f). These results are consistent with our *in vitro* study using primary cultured astrocytes (Fig. 1). In addition, similar to control astrocytes without viral transduction, mRFP-p130PH-expressing astrocytes did not exhibit spontaneous somatic $Ca^{2+}$ activity in the absence of ATP stimulation (Fig. 7f). Thus our data demonstrated the functional expression of p130PH in astrocytes *in vivo* by viral transduction.

## DISCUSSION

In this study, we transduced both the mouse cortex and hippocampus with serotype 2/5 rAAV vectors to introduce genes encoding the $IP_3$-binding protein p130PH and mRFP into astrocytes. Specific expression of transgenes in astrocytes was achieved by a novel astrocyte-specific GFAP promoter entitled gfa$ABC_1$D. Expression of the transgene could be readily observed by directly viewing the fluorescence of tag proteins in brain sections using confocal microscopy or in brains of live mice using 2-P microscopy. The transgene function was further assessed by *in vivo* 2-P $Ca^{2+}$ imaging. Our data clearly demonstrated that transgenes were exclusively expressed in astrocytes with little or low cellular toxicity, and ATP-stimulated $Ca^{2+}$ signals were significantly inhibited in mRFP-p130PH-expressing astrocytes.

rAAV vectors have been used increasingly to introduce transgenes into the CNS (Davidson and Breakefield, 2003; Davidson et al., 2000; Cearley and Wolfe, 2006; Cearley and Wolfe, 2007; Peel and Klein, 2000). However, the majority of these studies were designed to characterize the transduction efficiency and tropism of different serotypes of rAAV vectors by examining the expression of report fluorescence proteins GFP and DsRed. Most AAV

serotypes reported in the literature have preferential neuronal tropism *in vivo*. rAAV5 was shown to introduce report genes into both neurons and glial cells in the brain under control of the Rous sarcoma virus (RSV) promoter (Tenenbaum et al., 2004; Davidson et al., 2000), but it transduced neither neurons or astrocytes under control of the murine cytomegalovirus (mCMV) immediate-early promoter (Shevtsova et al., 2005). Thus, the capsid sequence and the promoter together determine the cellular expression pattern of transgenes. Recently, methods for pseudotyping rAAV vectors have been developed. The *rep* gene of AAV2 was widely used to pseudotype with the *cap* gene of other serotypes of AAV (Burger et al., 2004; Cearley and Wolfe, 2007; Cearley and Wolfe, 2006). Discrepancies regarding the tropism of pseudo-type rAAV2/5 for astrocytes were also reported in various studies. No report gene expression was observed in astrocytes transduced by rAAV2/5 vectors with chicken β-actin (CBA) promoters (Burger et al., 2004), while rAAV2/5 vectors with CMV promoters exhibited tropism for astrocytes (Halassa et al., 2007; Davidson et al., 2000). The discrepancy might have been due to the use of different promoters rather than the tropism of rAAV2/5. Although a neuronal promoter was used in some studies to introduce transgenes into neurons, previous attempts to use the astrocyte-specific GFAP promoter gfa2 (a 2.2 kb promoter) to selectively introduce genes into astrocytes using the pTR/UF AAV vectors have not been consistent (Peel and Klein, 2000; Feng et al., 2004). Furthermore, lentiviral vectors encoding transgene GFP under a gfa2 promoter do not produce a high expression level of GFP (Jakobsson et al., 2003; Jakobsson et al., 2004). These studies suggest that the gfa2 promoter might be problematic for use in viral transduction. In our study, we inserted a novel and smaller GFAP promoter gfaABC$_1$D (Lee et al., 2008) into the *cis*-expressing vector and tested the cellular specificity of transgene expression. This promoter also has the advantage of allowing larger transgene to be inserted into the vector.

We have demonstrated in several ways that mRFP-p130PH-expressing cells driven by the gfaABC$_1$D promoter are indeed astrocytes. First, morphologically, these cells have fine bush-like processes extending from the main processes, a feature characteristic of astrocytes *in vivo*. Second, many cells have terminal processes (end feet) surrounding blood vessels, which is another feature of astrocytes. Third, 94.7% and 93.2% of GFAP+ astrocytes express mRFP-p130PH in the cortex and hippocampus, while not a single mRFP-p130PH-expressing cell in transduced regions was NeuN+, Iba1+, CNPase+ and NG2+, markers for mature and healthy neurons, microglia, oligodendrocytes and NG2 cells, respectively. Finally, mRFP fluorescence is colocalized with fluo-4 labeled astrocytes. The expression of transgenes can be directly observed by viewing fusion protein fluorescence through confocal and 2-P microscopy, indicating a high expression level of the transgene *in vivo*. Thus, using rAAV2/5 with a gfaABC$_1$D promoter, we can exclusively introduce transgenes into astrocytes with high transduction efficiency and expression levels, providing an approach that can manipulate gene expression in astrocytes *in vivo*.

Although AAV has been considered to be a non-toxic, high titer injection of AAV could still cause astrocytic gliosis (Ortinski et al., 2010). Here we assessed possible transduction-induced cellular toxicity using immunocytochemistry and by examining the time-dependent changes in the cell densities of neurons and astrocytes. Based on GFAP and Iba1 staining, we observed that reactive astrocytes and microglia only exist around the injection site and dorsal surface of the cortex, but not in the region distant from the injection site where transduced astrocytes still can be identified by mRFP fluorescence. We demonstrated similar neuronal densities in transduced and non-transduced regions over post-transduction times for up to 10 weeks, suggesting no cellular toxicity was caused by the rAAV2/5 transduction. Astrocyte densities in transduced regions were also stable. Consequently, these results led us to conclude that the expression of mRFP-p130PH in astrocytes transduced by rAAV2/5 under control of the astrocyte-specific ABC$_1$D promoter cause little or no neuronal and glial toxicity *in vivo*.

p130PH acts as a mobile cytosolic $IP_3$ 'sponge' and thus can inhibit $Ca^{2+}$ release from internal store by reducing the concentration of free $IP_3$, the second messenger for mobilizing $Ca^{2+}$ from internal store (Lin et al., 2005). From an *in vitro* binding assay, it was reported that p130PH had an $IC_{50}$ value of 22 nM (Varnai et al., 2002). Since resting astrocytes are quiescent in $Ca^{2+}$ activity, the concentrations of $IP_3$ are expectedly very low. Since activation of the P2Y receptor by ATP has been shown to stimulate a dramatic increase in $IP_3$ release (Lin et al., 2005), the reduction of the $Ca^{2+}$ signal to ~28% in p130PH-expressing astrocytes after ATP stimulation is in agreement with the buffering effect of p130PH. Other $Ca^{2+}$ binding proteins such as the $IP_3R$ binding domain may also serve as a $IP_3$ sponge to reduce $Ca^{2+}$ release (Lin et al., 2005;Varnai et al., 2002). Finally, the $IP_3$ 5-phosphatase, an enzyme that can specifically hydrolyze $IP_3$, may exhibit a higher capacity to suppress the $Ca^{2+}$ signal than $IP_3$ sponges (Kanemaru et al., 2007).

The present study not only demonstrated specific transduction of the transgene in astrocytes, but also examined the functionality of transduced genes using *in vivo* imaging. $Ca^{2+}$ imaging using 2-P microscopy showed that the ATP-induced $Ca^{2+}$ signal was significantly reduced in mRFP-p130PH-expressing astrocytes, consistent with the results obtained from *in vitro* primary cultured astrocytes. Given the importance of astrocytic $Ca^{2+}$ signaling *in vivo*, our approach will provide an alternative tool to inhibit astrocytic $Ca^{2+}$ in neuron-glia interactions, and to specifically introduce transgenes into astrocytes in general. Our previous studies showed that the increased astrocytic $Ca^{2+}$ signals contribute to neurotoxicity after status epilepticus and focal ischemia (Ding et al., 2007; Ding et al., 2009). Introduction of p130PH using this viral approach will be a good tool to investigate whether disruption of the $Ca^{2+}$ signaling pathway may reduce brain damage in neurological diseases. In the CNS, other neurodegenerative diseases such as amyotrophic lateral sclerosis are caused by glial cell malfunction, thus selective introduction of transgenes into astrocytes to restore gene function might provide a therapeutic avenue that can ameliorate neurodegeneration. A recent study reported selective expression of GFP in astrocytes by transduction of serotypes 8 and rh43 of AAV using a cell-specific promoter; however, a functional study was not performed (Lawlor et al., 2009). Several new serotypes of the rAAV vector with CMV promoter have been reported to have astrocytic tropism in white matter, although with low transduction efficiency (Cearley et al., 2008). Because those vectors have relatively large transduced volume in the brain, it will be of interest to investigate whether these serotypes with a glial promoter may be effective to treat astrocyte-related neurodegenerative diseases.

*In summary*, our study demonstrated that transgenes can be exclusively introduced into astrocytes *in vivo* using rAAV2/5 vectors under the control of a novel glia-specific promoter. High transduction efficiency of rAAV2/5 indicates a preferential receptor tropism of the serotype 5 capsid. Furthermore, *in vivo* $Ca^{2+}$ imaging showed that astrocytes expressing the transgene had reduced $Ca^{2+}$ elevation in response to ATP stimulation. Thus, rAAV2/5 vectors containing a novel astrocyte-specific promoter provided an efficient tool to selectively inhibit astrocytic $Ca^{2+}$ signaling. Furthermore, a method to introduce transgenes into glial cell types in the brain allows future studies to examine neuron-glia interactions and potential treatment of astrocyte-related CNS diseases.

## Acknowledgments

Support for this project was provided by grants from the American Heart Association (0735133N), R01NS069726 from NIH, Ralph E. Powe Junior Faculty Award (FY2008-206) from Oak Ridge Associated Universities, and startup funds to SD, and P01 AG018357 from NIH to GYS. We would like to acknowledge the Gene Therapy Resource Program (GTRP) of the National Heart, Lung, and Blood Institute (NIHLBI) for providing the gene vectors used in this study. We appreciate the work done by the University of Pennsylvania Vector Core in conducting the vector production through the GTRP program. We would like to thank Dr. Mike Brenner for providing DNA constructs of gfaABC$_1$D promoter. The authors also thank Cynthia Haydon and Dennis Reith for the critical reading and editing of this manuscript and Cindy Chu and Min Li for their assistance in molecular

biology. Confocal images were acquired with an Olympus FV1000 confocal microscope purchased by NIH shared instrument grant (RR022578).

## REFERENCES

Angulo MC, Kozlov AS, Charpak S, Audinat E. Glutamate released from glial cells synchronizes neuronal activity in the hippocampus. J Neurosci. 2004; 24:6920–6927. [PubMed: 15295027]

Burger C, Gorbatyuk OS, Velardo MJ, Peden CS, Williams P, Zolotukhin S, Reier PJ, Mandel RJ, Muzyczka N. Recombinant AAV Viral Vectors Pseudotyped with Viral Capsids from Serotypes 1, 2, and 5 Display Differential Efficiency and Cell Tropism after Delivery to Different Regions of the Central Nervous System. Mol Ther. 2004; 10:302–317. [PubMed: 15294177]

Cearley CN, Vandenberghe LH, Parente MK, Carnish ER, Wilson JM, Wolfe JH. Expanded Repertoire of AAV Vector Serotypes Mediate Unique Patterns of Transduction in Mouse Brain. Mol Ther. 2008

Cearley CN, Wolfe JH. Transduction Characteristics of Adeno-associated Virus Vectors Expressing Cap Serotypes 7, 8, 9, and Rh10 in the Mouse Brain. Mol Ther. 2006; 13:528–537. [PubMed: 16413228]

Cearley CN, Wolfe JH. A Single Injection of an Adeno-Associated Virus Vector into Nuclei with Divergent Connections Results in Widespread Vector Distribution in the Brain and Global Correction of a Neurogenetic Disease. J Neurosci. 2007; 27:9928–9940. [PubMed: 17855607]

D'Ascenzo M, Fellin T, Terunuma M, Revilla-Sanchez R, Meaney DF, Auberson YP, Moss SJ, Haydon PG. mGluR5 stimulates gliotransmission in the nucleus accumbens. PNAS. 2007; 104:1995–2000. [PubMed: 17259307]

Davidson BL, Stein CS, Heth JA, Martins I, Kotin RM, Derksen TA, Zabner J, Ghodsi A, Chiorini JA. Recombinant adeno-associated virus type 2, 4, and 5 vectors: transduction of variant cell types and regions in the mammalian central nervous system. Proceedings of the National Academy of Sciences of the United States of America. 2000; 97:3428–3432. [PubMed: 10688913]

Davidson BL, Breakefield XO. Viral vectors for gene delivery to the nervous system. Nat Rev Neurosci. 2003; 4:353–364. [PubMed: 12728263]

Ding S, Wang T, Cui W, Haydon PG. Photothrombosis ischemia stimulates a sustained astrocytic $Ca^{2+}$ signaling in vivo. GLIA. 2009; 57:767–776. [PubMed: 18985731]

Ding S, Fellin T, Zhu Y, Lee SY, Auberson YP, Meaney DF, Coulter DA, Carmignoto G, Haydon PG. Enhanced Astrocytic $Ca^{2+}$ Signals Contribute to Neuronal Excitotoxicity after Status Epilepticus. J Neurosci. 2007; 27:10674–10684. [PubMed: 17913901]

Erb L, Liao Z, Seye CI, Weisman GA. P2 receptors: intracellular signaling. Pflugers Archiv - European Journal of Physiology. 2006; 452:552–562. [PubMed: 16586093]

Fellin T, Pascual O, Gobbo S, Pozzan T, Haydon PG, Carmignoto G. Neuronal synchrony mediated by astrocytic glutamate through activation of extrasynaptic NMDA receptors. Neuron. 2004; 43:729–743. [PubMed: 15339653]

Feng X, Eide FF, Jiang H, Reder AT, Feng X, Eide FF, Jiang H, Reder AT. Adeno-associated viral vector-mediated ApoE expression in Alzheimer's disease mice: low CNS immune response, long-term expression, and astrocyte specificity. Frontiers in Bioscience. 2004; 9:1540–1546. [PubMed: 14977565]

Fiacco TA, Agulhon C, Taves SR, Petravicz J, Casper KB, Dong X, Chen J, McCarthy KD. Selective Stimulation of Astrocyte Calcium In Situ Does Not Affect Neuronal Excitatory Synaptic Activity. Neuron. 2007; 54:611–626. [PubMed: 17521573]

Fisher KJ, Jooss K, Alston J, Yang Y, Haecker SE, High K, Pathak R, Raper SE, Wilson JM. Recombinant adeno-associated virus for muscle directed gene therapy. Nat Med. 1997; 3:306–312. [PubMed: 9055858]

Gunnarson E, Axehult G, Baturina G, Zelenin S, Zelenina M, Aperia A. Identification of a molecular target for glutamate regulation of astrocyte water permeability. GLIA. 2008; 56:587–596. [PubMed: 18286643]

Halassa MM, Fellin T, Takano H, Dong JH, Haydon PG. Synaptic Islands Defined by the Territory of a Single Astrocyte. J Neurosci. 2007; 27:6473–6477. [PubMed: 17567808]

Haydon PG. GLIA: listening and talking to the synapse. Nature Reviews Neuroscience. 2001; 2:185–193.

Haydon PG, Carmignoto G. Astrocyte Control of Synaptic Transmission and Neurovascular Coupling. Physiol Rev. 2006; 86:1009–1031. [PubMed: 16816144]

Hirase H, Qian L, Bartho P, Buzsaki G. Calcium dynamics of cortical astrocytic networks *in vivo*. Plos Biology. 2004; 2:E96. [PubMed: 15094801]

Jakobsson J, Ericson C, Jansson M, Bjork E, Lundberg C. Targeted transgene expression in rat brain using lentiviral vectors. Journal of Neuroscience Research. 2003; 73:876–885. [PubMed: 12949915]

Jakobsson J, Georgievska B, Ericson C, Lundberg C. Lesion-dependent regulation of transgene expression in the rat brain using a human glial fibrillary acidic protein-lentiviral vector. European Journal of Neuroscience. 2004; 19:761–765. [PubMed: 14984426]

Kanemaru K, Okubo Y, Hirose K, Iino M. Regulation of Neurite Growth by Spontaneous $Ca^{2+}$ Oscillations in Astrocytes. J Neurosci. 2007; 27:8957–8966. [PubMed: 17699677]

Lawlor PA, Bland RJ, Mouravlev A, Young D, During MJ. Efficient Gene Delivery and Selective Transduction of Glial Cells in the Mammalian Brain by AAV Serotypes Isolated From Nonhuman Primates. Mol Ther. 2009; 17:1692–1702. [PubMed: 19638961]

Lee Y, Messing A, Su M, Brenner M. GFAP promoter elements required for region-specific and astrocyte-specific expression. GLIA. 2008; 56:481–493. [PubMed: 18240313]

Li X, Zima AV, Sheikh F, Blatter LA, Chen J. Endothelin-1-Induced Arrhythmogenic $Ca^{2+}$ Signaling Is Abolished in Atrial Myocytes of Inositol-1,4,5-Trisphosphate($IP_3$)-Receptor Type 2-Deficient Mice. Circ Res. 2005; 96:1274–1281. [PubMed: 15933266]

Lin X, Varnai P, Csordas G, Balla A, Nagai T, Miyawaki A, Balla T, Hajnoczky G. Control of Calcium Signal Propagation to the Mitochondria by Inositol 1,4,5-Trisphosphate-binding Proteins. J Biol Chem. 2005; 280:12820–12832. [PubMed: 15644334]

Liu F, You Y, Li X, Ma T, Nie Y, Wei B, Li T, Lin H, Yang Z. Brain Injury Does Not Alter the Intrinsic Differentiation Potential of Adult Neuroblasts. J Neurosci. 2009; 29:5075–5087. [PubMed: 19386903]

McCarthy KD, de Vellis J. Preparation of separate astroglial and oligodendroglial cell cultures from rat cerebral tissue. J Cell Biol. 1980; 85:890–902. [PubMed: 6248568]

Ni Y, Malarkey EB, Parpura V. Vesicular release of glutamate mediates bidirectional signaling between astrocytes and neurons. Journal of Neurochemistry. 2007; 103:1273–1284. [PubMed: 17727631]

Nimmerjahn A, Kirchhoff F, Kerr JN, Helmchen F. Sulforhodamine 101 as a specific marker of astroglia in the neocortex in vivo. Nature Methods. 2004; 1:31–37. [PubMed: 15782150]

Ortinski PI, Dong J, Mungenast A, Yue C, Takano H, Watson DJ, Haydon PG, Coulter DA. Selective induction of astrocytic gliosis generates deficits in neuronal inhibition. Nat Neurosci. 2010; 13:584–591. [PubMed: 20418874]

Parpura V, Basarsky TA, Liu F, Jeftinija K, Jeftinija S, Haydon PG. Glutamate-mediated astrocyte-neuron signalling. Nature. 1994; 369:744–747. [see comment]. [PubMed: 7911978]

Peel AL, Klein RL. Adeno-associated virus vectors: activity and applications in the CNS. Journal of Neuroscience Methods. 2000; 98:95–104. [PubMed: 10880823]

Petravicz J, Fiacco TA, McCarthy KD. Loss of $IP_3$ Receptor-Dependent $Ca^{2+}$ Increases in Hippocampal Astrocytes Does Not Affect Baseline CA1 Pyramidal Neuron Synaptic Activity. J Neurosci. 2008; 28:4967–4973. [PubMed: 18463250]

Shevtsova Z, Malik JMI, Michel U, Bahr M, Kugler S. Promoters and serotypes: targeting of adeno-associated virus vectors for gene transfer in the rat central nervous system in vitro and *in vivo*. Exp Physiol. 2005; 90:53–59. [PubMed: 15542619]

Sofroniew MV. Reactive Astrocytes in Neural Repair and Protection. Neuroscientist. 2005; 11:400–407. [PubMed: 16151042]

Takano T, Tian GF, Peng W, Lou N, Libionka W, Han X, Nedergaard M. Astrocyte-mediated control of cerebral blood flow. Nat Neurosci. 2006; 9:260–267. [PubMed: 16388306]

Tenenbaum L, Chtarto A, Lehtonen E, Velu T, Brotchi J, Levivier M. Recombinant AAV-mediated gene delivery to the central nervous system. Journal of Gene Medicine. 2004; 6 Suppl 1:S212–S222. [PubMed: 14978764]

Tian GF, Azmi H, Takano T, Xu Q, Peng W, Lin J, Oberheim N, Lou N, Wang X, Zielke HR, Kang J, Nedergaard M. An astrocytic basis of epilepsy. Nature Medicine. 2005; 11:973–981.

Varnai P, Lin X, Lee SB, Tuymetova G, Bondeva T, Spat A, Rhee SG, Hajnoczky G, Balla T. Inositol Lipid Binding and Membrane Localization of Isolated Pleckstrin Homology (PH) Domains. STUDIES ON THE PH DOMAINS OF PHOSPHOLIPASE C delta 1 AND p130. J Biol Chem. 2002; 277:27412–27422. [PubMed: 12019260]

Wang X, Lou N, Xu Q, Tian GF, Peng WG, Han X, Kang J, Takano T, Nedergaard M. Astrocytic $Ca^{2+}$ signaling evoked by sensory stimulation in vivo. Nature Neuroscience. 2006; 9:816–823.

Wilhelmsson U, Bushong EA, Price DL, Smarr BL, Phung V, Terada M, Ellisman MH, Pekny M. Redefining the concept of reactive astrocytes as cells that remain within their unique domains upon reaction to injury. Proceedings of the National Academy of Sciences of the United States of America. 2006; 103:17513–17518. [PubMed: 17090684]

Zhang W, Xie Y, Wang T, Bi J, Li H, Zhang LQ, Ye SQ, Ding S. Neuronal Protective Role of PBEF in a Mouse Model of Cerebral Ischemia. J Cerebral Blood Flow and Metabolism. 2010 (On line publication, May 19, 2010).

Zhu D, Lai Y, Shelat PB, Hu C, Sun GY, Lee JCM. Phospholipases A2 Mediate Amyloid-beta Peptide-Induced Mitochondrial Dysfunction. J Neurosci. 2006; 26:11111–11119. [PubMed: 17065451]

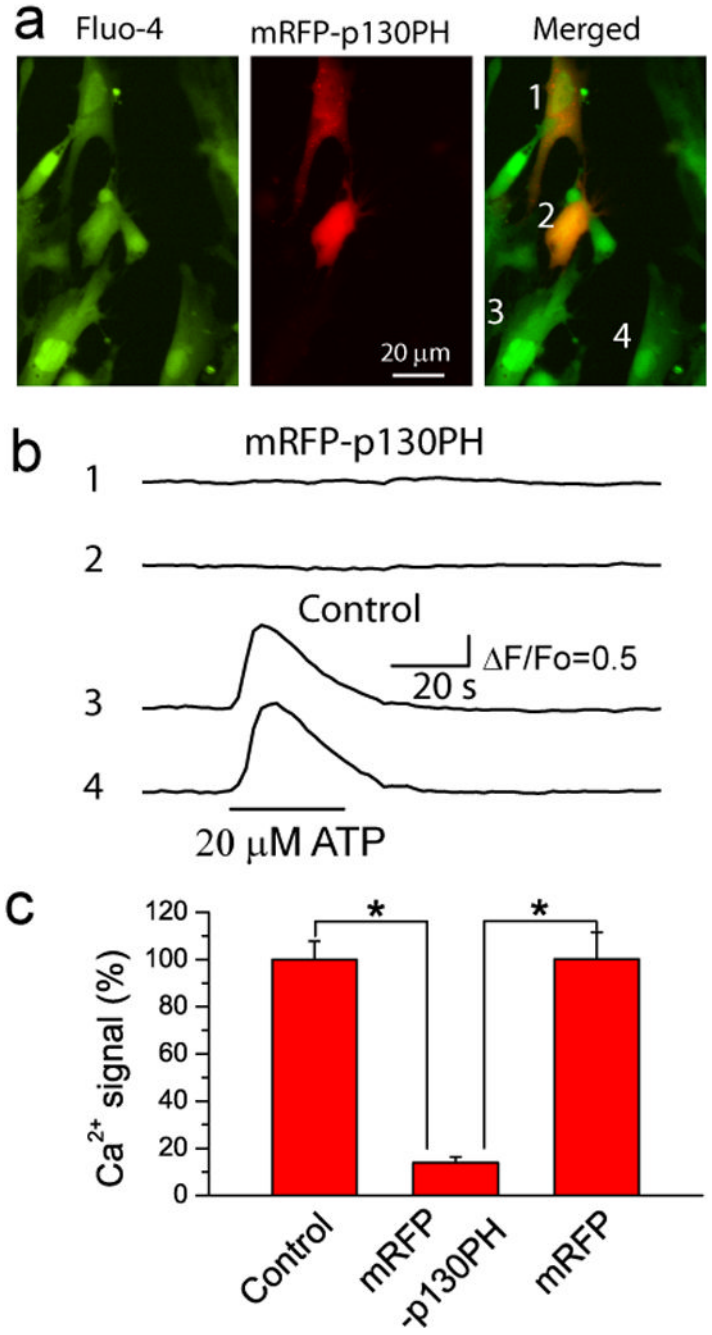


**Fig. 1. Expression of p130PH inhibited $Ca^{2+}$ signal in primary cultured astrocytes**

(a) Epi-fluorescence images of fluo-4 (left) and mRFP-p130PH (middle) fluorescence in astrocytes. Notice that astrocytes 1 and 2 were transfected with mRFP-p130PH. (b) Time courses of astrocytic $Ca^{2+}$ elevations in response to ATP stimulation in transfected (1 and 2) and non-transfected (3 and 4) astrocytes shown in A. (c) Summary of $Ca^{2+}$ signals stimulated by 20 μM ATP from astrocytes with transfection of mRFP-p130PH (n=15 cells) and mRFP (n=10 cells), and without transfection (control, n=42 cells). Data was normalized to control astrocytes. All data was collected from 3–4 preparations of primary cultured astrocytes. *$p$<0.0005, t-test.

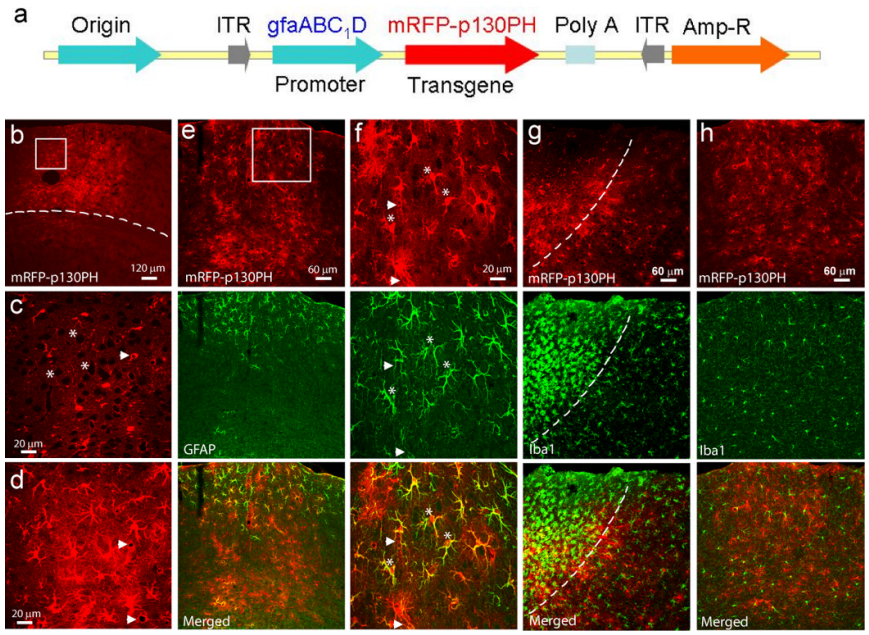


**Fig. 2. Construction of viral plasmid and transgene expression after viral transduction in the brain**

(a) Linear feature map of expressing plasmid of rAAV2/5 vector. The plasmid contained an astrocyte-specific GFAP promoter gfaABC$_1$D and transgene p130PH with fusion protein mRFP. Poly A: SV40 late polyadenylation signal sequence. ITR: inverted terminal repeat at the end of viral genome, which is required for replication. (b–d) Confocal images of mRFP-p130PH+ cells in the transduced region in the cortex in a coronal section. (b) Low-resolution maximal projection image. (c–d) A single optical section (c) and a maximal projection image (d) from the boxed region in (b). Note the black spots (indicated by *) in (c) and the blood vessels in (c–d) (arrow heads) surrounded by mRFP fluorescence. The cortical region is located above the dash line in (b). (e–f) Maximal projection images of mRFP-p130PH fluorescence and GFAP signal in a transduced region of a coronal brain section with low (e) and high (f) resolution. Image in (f) is from the boxed region of (e). Notice the colocalization of GFAP and mRFP signals near the cortical surface (some cells were indicated by * in (f)) and low GFAP expression level in deeper layers of the cortex (e). The blood vessels surrounded by terminal processes are indicated by arrow head in (f). (g) Iba 1 staining of a transduced region including injection site. The dashed line separates the region having reactive microglia (left) from the region having normal microglia. (h) Iba 1 staining of a transduced region distant from injection site shows a normal morphology of microglia.

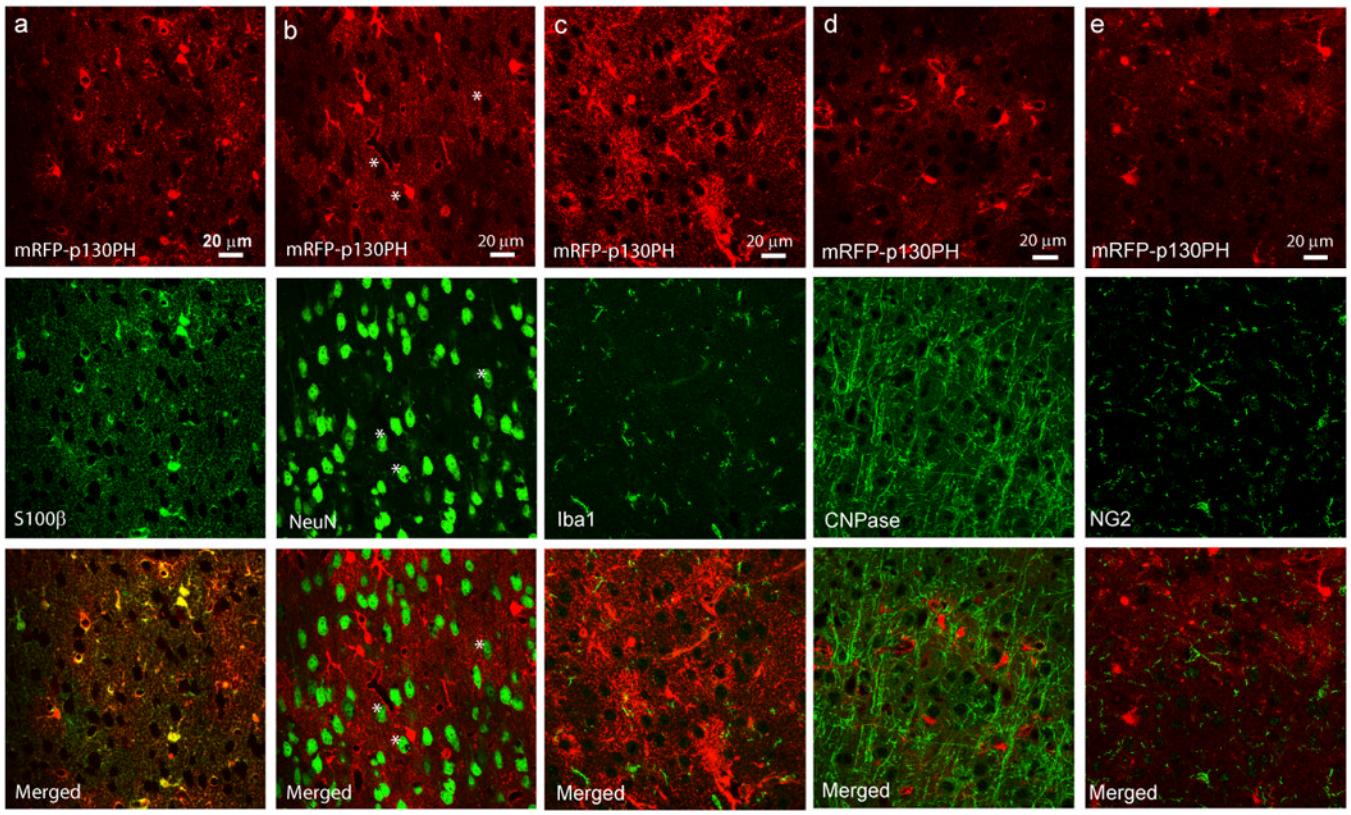


**Fig. 3. Selective expression of mRFP-p130PH in astrocytes in the cortex**

Single optical section images of mRFP-p130PH signal (top panels) and S100β (a), NeuN (b), Iba1 (c), CNPase (d) and NG2 (e) signals, and merged images (bottom panels). Notice the colocalization between S100β and mRFP signals in (a). The black spots surrounded by mRFP fluorescence in (b) are neuronal identities (*).

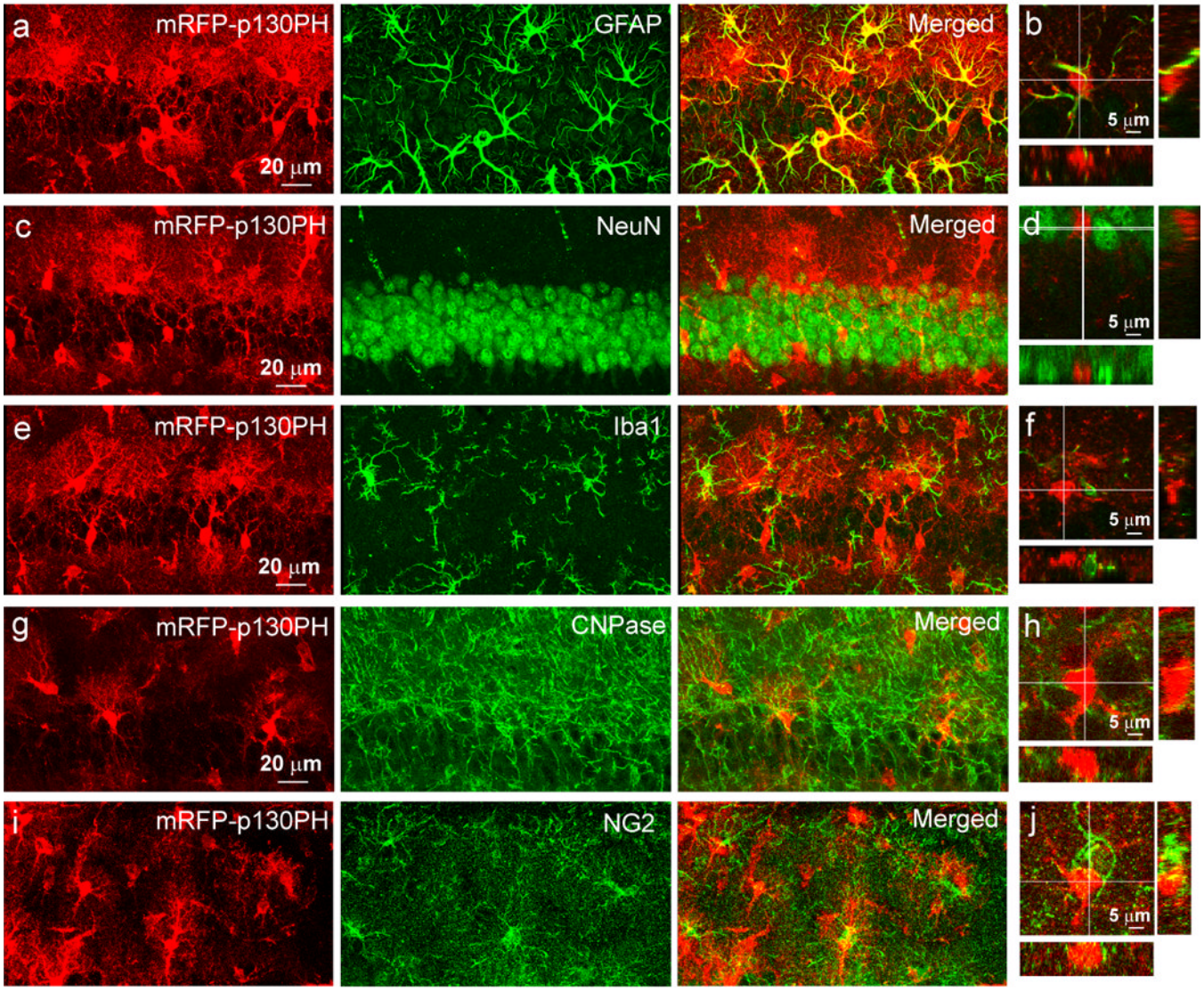


**Fig. 4. Selective expression of mRFP-p130PH in astrocytes in the hippocampus**

Maximal projection images of mRFP-p130PH expressing astrocytes in hippocampus CA1 regions stained with antibodies against GFAP (a), NeuN (c), Iba1 (e), CNPase (g) and NG2 (i), and their respective orthogonal analysis (b, d, f, h and j).

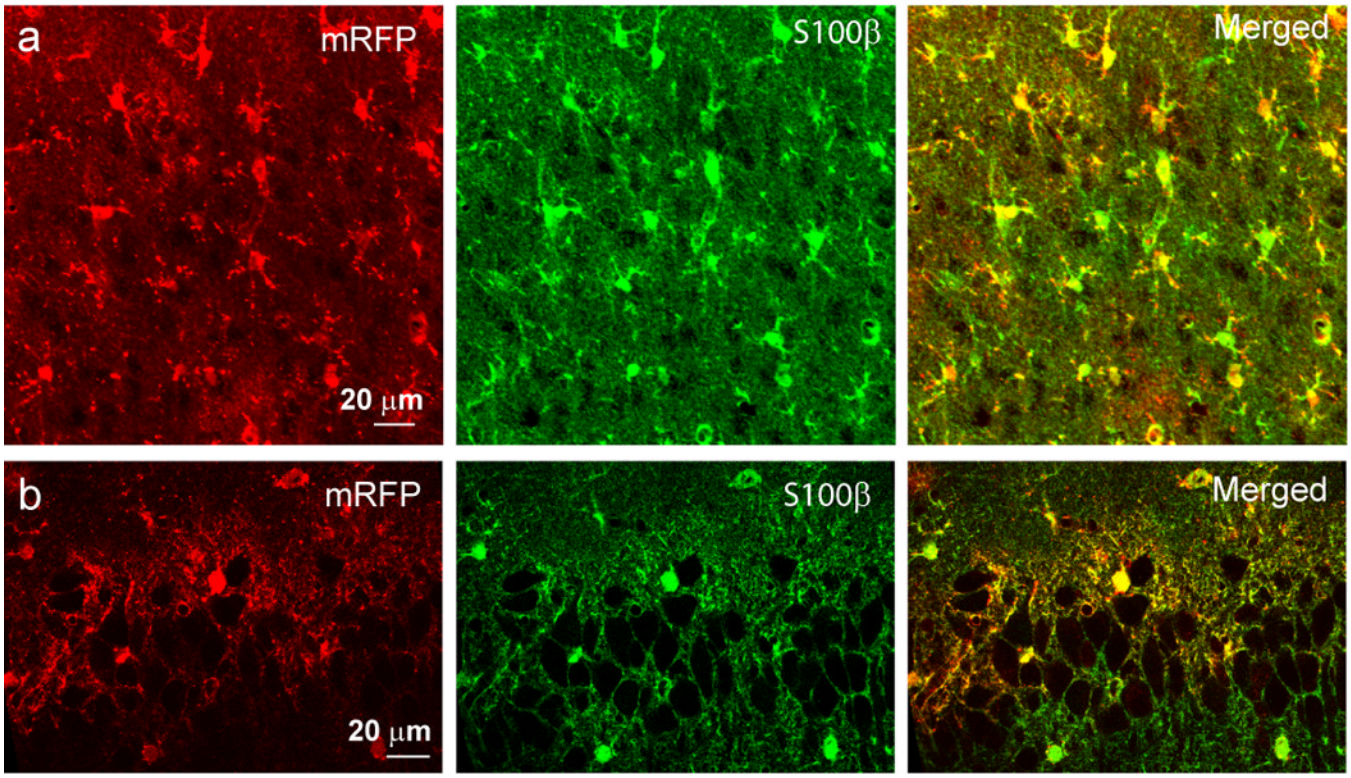


**Fig. 5. Selective expression of mRFP in astrocytes in the cortex and hippocampus**

(a–b) mRFP expressing astrocytes after viral transduction in the cortex (a) and hippocampus CA1 regions (b) stained with antibodies against S100β.

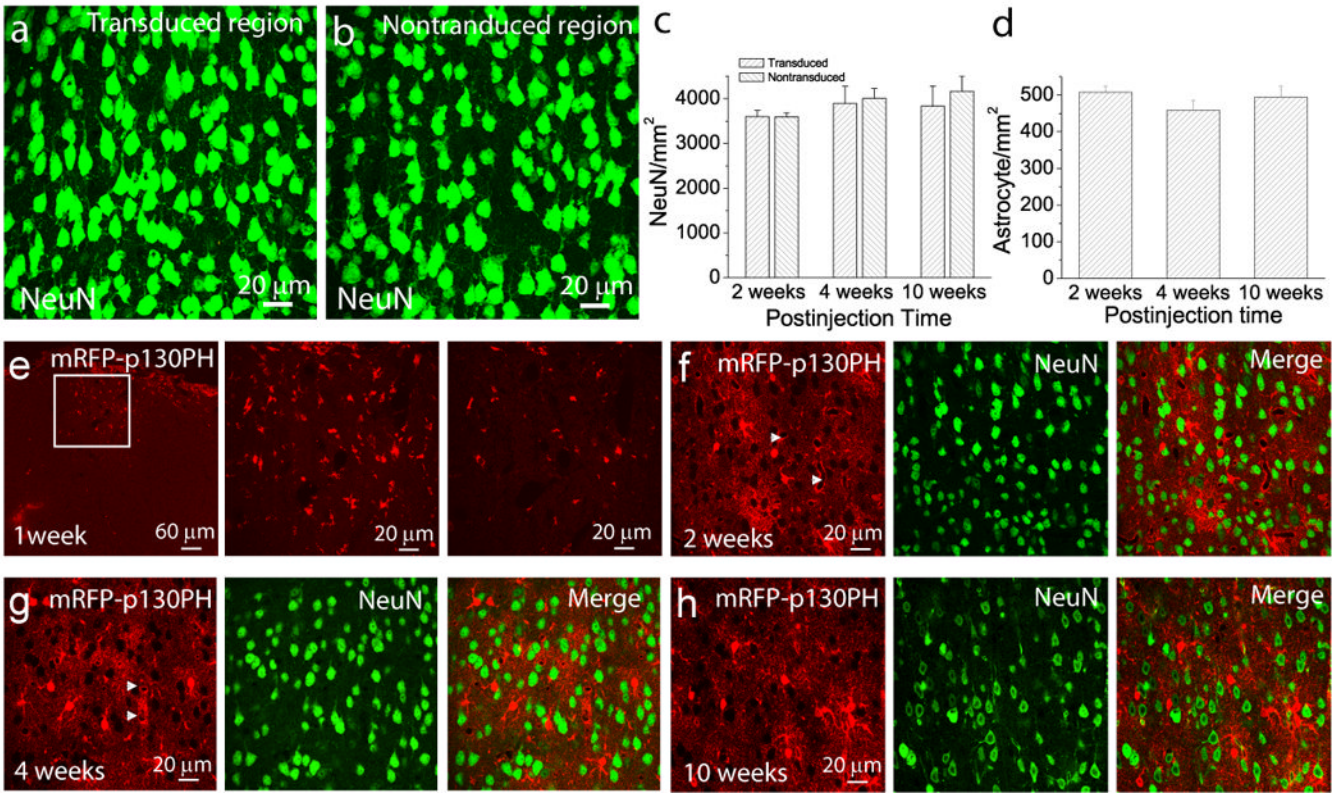


**Fig. 6. Evaluation of cellular toxicity and time-dependent expression of transgene following rAAV2/5 transduction**

(a–b) Maximal projection images of layer 2/3 neurons stained with anti-NeuN antibody in transduced (a) and non-transduced (b) regions in the cortex. (c) Densities of layer 2/3 NeuN + cortical neurons in transduced and non-transduced regions at different time points of post transduction. Data at each time point were collected from 7–11 brain sections of N=2–3 mice. (d) Densities of mRFP-p130PH-expressing astrocyte in the transduced region at different times following viral injection. Data from each time point were collected from 12–30 sections from N=2–4 mice. Since transgene was not fully expressed at 1 week after transduction, no data from this time point was included. (e) mRFP fluorescence in a brain section 1 week following viral injection. (Left) Maximal projection image with low resolution indicated the transduced region. (Middle) Maximal projection image with high resolution from the boxed region in the left panel revealed mRFP expression in individual cells. (Right) A single optical section of the middle panel. (f–h) Single optical section images of mRFP-p130PH expression (left) and NeuN signal (middle) in the cortex after 2, 4 and 10 weeks following viral injection. Notice the blood vessels surrounded by terminal processes (arrow heads) in (f) and (g).

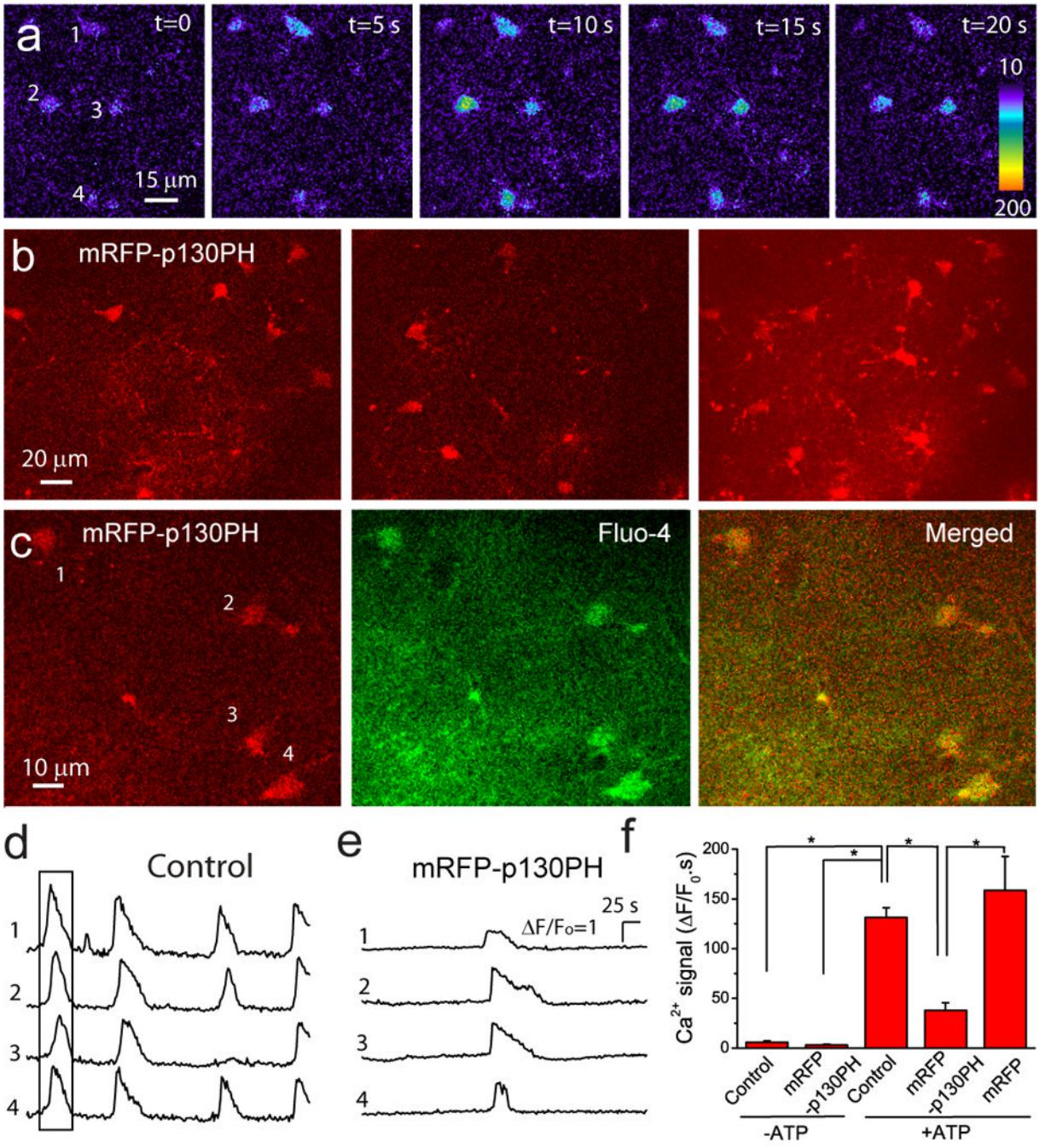


**Fig. 7. p130PH expression by viral transduction reduces ATP-stimulated $Ca^{2+}$ signal in the cortex *in vivo***

(a) Astrocytes in the cortex are labeled with fluo-4. (b) *In vivo* imaging of mRFP-p130PH-expressing astrocytes. Single frame images at 70 μm (left) and 95 μm (middle) deep from the surface of cortex and the maximal projection image (right) from a z-stake image from 60 μm to 100 μm deep of cortex with 1 μm step. (c) 2-P images of mRFP-p130PH-expressing astrocytes (left) labeled with fluo-4 (middle). The right panel is the merged image. (d–e) Representative time course of $Ca^{2+}$ signal in control (d) and mRFP-p130PH-expressing (e) astrocytes in response to 0.5 mM ATP. Four cells are from the same image frames in (a) and (c), respectively. The boxed region in (d) is corresponding to the images in (a). Astrocytes

were stimulated by 0.5 mM ATP. (f) Summary of astrocytic $Ca^{2+}$ signals from control (N=7), mRFP-p130PH-expressing (N=8), and mRFP-expressing (N=4) mice stimulated by 0.5 mM ATP, and mice without ATP stimulation (N=4 for uninjected mice and N=4 for mRFP-p130PH expressing mice). Mice 2–4 weeks after viral injection were used in this experiment. Data were collected from 15–25 astrocytes in each mouse and averaged as a single value for this mouse. *$p$<0.05, $t$test.